I&EC research
Industrial & Engineering Chemistry Research
pubs.acs.org/IECR
Article

Double-Layer Simulated Moving Bed Chromatography for Ternary Separations: Serialized Layer Configurations

Ju Weon Lee*

Cite This: *Ind. Eng. Chem. Res.* 2021, 60, 8911−8926

ABSTRACT: Double-layer simulated moving bed chromatography introduced for the complete ternary separation problems utilizes parallel column configurations. The inlet and outlet streams of paired columns need to be properly split and merged to realize parallel operations with the packed bed columns. To make a pair of split streams, at least one flow control unit is additionally required. Therefore, the double-layer simulated moving bed chromatography that consists of six zones with parallelized two columns required at least 10 pumps to control five internal flow splits and five external inlet and outlet flows. In this work, two alternative layer configurations of the double-layer simulated moving bed were introduced to simplify the internal flow patterns. Applying an orthogonal parameter screening method, the design parameters of the double-layer simulated moving bed processes were optimized. The simplified layer configurations were compared with the standard parallel double-layer configuration in terms of process performances and system pressure decrease.

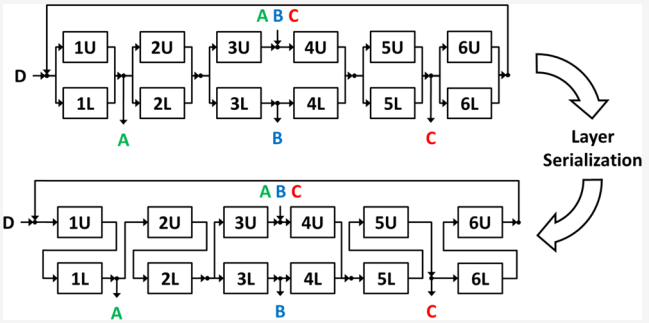

1. INTRODUCTION

Since the simulated moving bed (SMB) technology was introduced in the 1960s for binary and pseudo-binary separation problems, many modified SMB processes have been developed to improve the process performances for complex mixture separations.[1,2] By modulating the internal and external flow rates of the conventional four-zone SMB process, two well-established variations were introduced. The first one was called the outlet stream swing (OSS) operation.[3] In the OSS operation, the outlet flows were consecutively on and off to enhance the product qualities. The second one was developing well-posed internal concentration profiles by intermittent flow focusing of the external flows. Katsuo and Mazzotti introduced the intermittent-SMB with a two-step operation.[4] Lee et al. expanded this advanced operation concept to a generalized three-step flow-focusing operation.[5] Since the OSS and flow-focusing operations have more degrees of freedom in the operational aspect, these operations provided better performances than the conventional operation.[5]

The conventional four-zone SMB and its variations have a single-layer configuration, in which the columns are connected in series and form a single SMB ring. Therefore, most of the SMB process modifications for ternary separations were also developed with a single-layer configuration based on the conventional four-zone SMB. For example, the eight-zone SMB was composed of two integrated four-zone sub-SMBs in a single SMB ring.[6] One product stream of the first four-zone sub-SMB was internally recycled to the second four-zone sub-SMB as a feed. In the SMB cascade, two four-zone SMBs were connected in series and operated individually.[7] Similar to the eight-zone SMB, the first SMB isolated one of the most- or least-retained components and the rest two components were separated in the second SMB.

Recently, a double-layer SMB was introduced in analogy to dividing wall column distillation, as shown in Figure 1.[8] Even though the double-layer SMB formed a single SMB ring like the eight-zone SMB, it could use different sizes of the columns in each layer like the SMB cascade. Therefore, the double-layer SMB could provide better performance than the eight-zone SMB and the SMB cascade in certain separation problems, in which the intermediate-retained component retention was not extremely close to one of the other components. Two columns were in one zone and operated in parallel. In zones 1, 2, 5, and 6, two columns were handled as a single column (paired double-layer zones) so that the ratios of the mobile-phase flow to the simulated stationary phase should be the same in both layers. In other zones (divided double-layer zones), two layers were individually operated with different operating conditions.

Received: April 1, 2021
Revised: May 19, 2021
Accepted: May 26, 2021
Published: June 9, 2021

https://doi.org/10.1021/acs.iecr.1c01268
Ind. Eng. Chem. Res. 2021, 60, 8911−8926

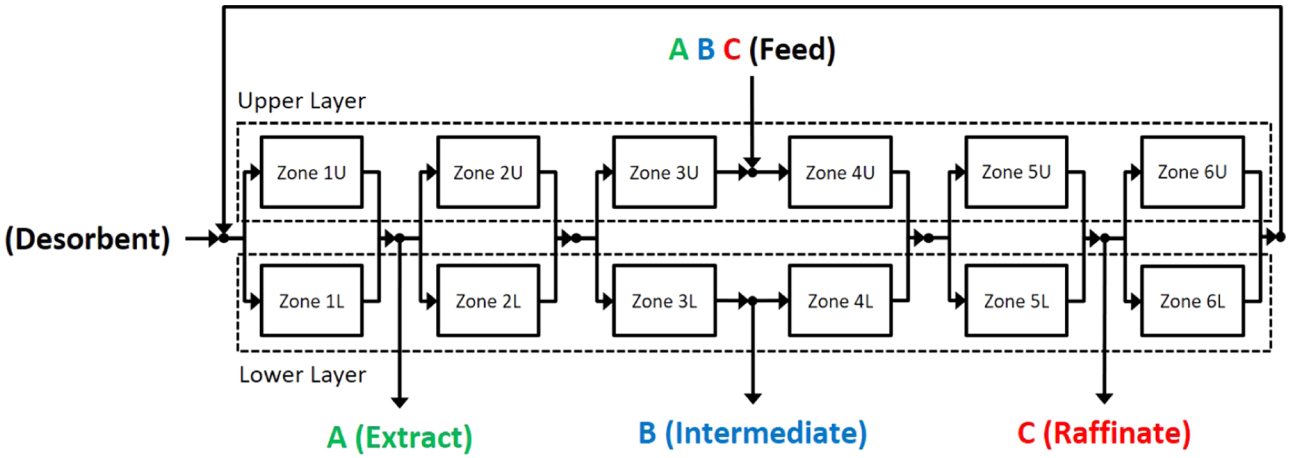

Figure 1. Schematic flow diagram and zone configuration of the parallel double-layer SMB process for ternary separations. U, upper layer; L, lower layer; Feed: feed stream; Dsrb, desorbent stream; Extr, extract stream; Intm, intermediate stream; Raff, raffinate stream; A, more-retained component; B, intermediate-retained component; and C, less-retained component.

Therefore, the layer outlet flows in the preceding zone merged and then split into the inlet flows of the following zone layers according to the volumes of the upper- and lower-layer columns. To control internal and external flows, five flow split units for internal flow splits and five flow control units for external inlets (feed and desorbent) and outlets (extract, intermediate, and raffinate) were required. At least 12 columns and 10 pumps (if all flows are controlled with a pump) were required to form a parallel double-layer SMB. Compared to other ternary SMB processes discussed above, such as the eight-zone SMB (eight columns and seven pumps) and the SMB cascade (eight columns and eight pumps), it requires high investment to be established.

In this work, two alternative layer configurations of the double-layer SMB, which adapted serialized column connections and step operations, were introduced to simplify the complex flow patterns of the parallel double-layer SMB. Assuming that all design parameters are orthogonal, the design parameters were screened to obtain the optimized process performance including the system pressure drop.

2. DESIGN OF DOUBLE-LAYER SMBS WITH VARIOUS LAYER CONFIGURATIONS

2.1. Parallel Double-Layer SMB: The Standard Layer Configuration. To determine the operating conditions of the double-layer SMB, a well-established SMB short-cut design method, the "triangle method", was applied.[9] The operating conditions of the SMB zones were determined by the ratio of the mobile-phase flow rate to the simulated stationary-phase flow rate (m-value),

$$m_j = \frac{Q_j - \varepsilon_T V_C/t_S}{(1-\varepsilon_T)V_C/t_S} \quad (1)$$

where m is the flow rate ratio, Q is the volumetric flow rate of the liquid phase, ε_T is the total void fraction of the column ($=\varepsilon_I + (1-\varepsilon_I)\varepsilon_P$), ε_I and ε_P are respectively the inter- and intraparticle void fractions of the column, t_S is the port switching interval, V_C is the empty column volume, and the subscript j denotes the zone j. To extend the triangle method into the double-layer SMB, a modified short-cut design method was introduced in the previous work.[8]

In principle, the layers of the double-layer SMB can be operated with different m-values. However, the roles of both layers are the same in the paired double-layer zones:

- Zone 1: eliminating the more-retained component to regenerate the stationary phase.
- Zone 2: eliminating the intermediate-retained component to avoid the extract port contamination.
- Zone 5: holding the intermediate-retained component to avoid the raffinate port contamination.
- Zone 6: holding the less-retained component to regenerate the mobile phase.

Eventually, both layers in the paired double-layer zones can share the same m-value by handling them as a single zone.

On the contrary, there is no internal flow split or mixing at the feed/intermediate ports so that both layers in the divided double-layer zones have distinct roles:

- Zone 3U: eliminating the less-retained component to avoid the intermediate port contamination through the zone 3L.
- Zone 4U: holding the more-retained component to avoid the intermediate port contamination through the zone 4L.
- Zone 3L: holding the more-retained component to avoid the intermediate port contamination.
- Zone 4L: eliminating the less-retained component to avoid the intermediate port contamination.

This means that both layers cannot be handled as a single zone. To decide the operating conditions of the double-layer SMB for complete ternary separations, eight m-values should be determined satisfying the following inequality conditions for a linear isotherm system:

$$K_C < m_{3U} < m_{4U} < K_A \quad (2)$$

$$K_C < m_{4L} < K_B < m_{3L} < K_A \quad (3)$$

$$K_C < m_5 < K_B < m_2 < K_A \quad (4)$$

$$m_6 < K_C,\ K_A < m_1 \quad (5)$$

where K is the partition coefficient; the subscripts U and L respectively denote the upper and lower layers; and the subscripts A, B, and C denote the more-, intermediate-, and less-retained components, respectively. Four operating points (m_1, m_6), (m_2, m_5), (m_{3U}, m_{4U}), and (m_{3L}, m_{4L}) can be drawn on

https://doi.org/10.1021/acs.iecr.1c01268
Ind. Eng. Chem. Res. 2021, 60, 8911−8926

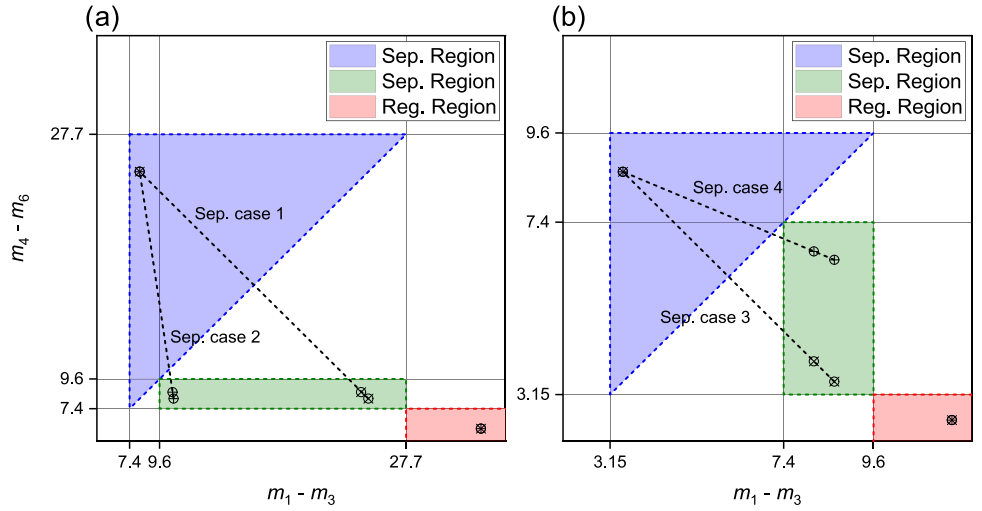

Figure 2. Separation (blue and green) and regeneration (red) regions of the double-layer SMB for the complete ternary separation. (a) dA/dT/dG separation, K_{dA} = 27.7, K_{dG} = 9.6, K_{dT} = 7.4 and (b) dT/dG/dC K_{dT} = 9.6, K_{dG} = 7.4, K_{dC} = 3.15. Linear isotherms; circles with × center, operating points with biggest m_2 or m_5 values; circles with + center, operating points with smallest m_2 or m_5 values; operating points in the blue separation regions, (m_{3U}, m_{4U}); operating points in the green separation regions, (m_{3L}, m_{4L}); operating points between (m_{3U}, m_{4U}) and (m_{3L}, m_{4L}), (m_2, m_5); and operating points in the red regeneration regions, (m_1, m_6).

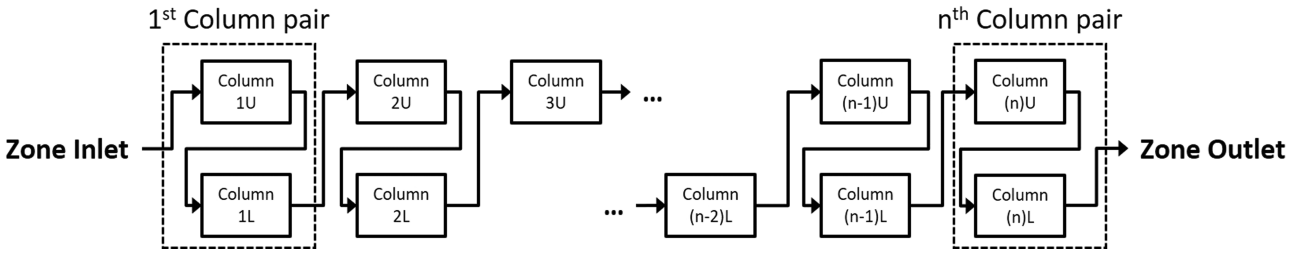

Figure 3. Serialized column connection of the paired double-layer zone: upper-to-lower serial connection.

the m-value plane, as shown in Figure 2. For the complete regeneration of the mobile and stationary phases, the operating point (m_1, m_6) should be in the red regeneration region, cf. eq 5. For the complete separation of the more- and less-retained components in zones 3U and 4U, the operating point (m_{3U}, m_{4U}) should be in the blue triangle separation region, cf. eq 2. To isolate the intermediate-retained component, the operating points (m_{3L}, m_{4L}) and (m_2, m_5) should be in the green rectangular separation region, cf. eqs 3 and 4.

The zone 2 outlet flow, the merged outlet flow of zones 2U and 2L, splits into two flows for the inlets of the zones 3U and 3L, and zone 4U and 4L outlet flows merge into a single flow for the zone 5 inlet, which is also split into two inlet flows for zones 5U and 5L. Therefore, the m-values for zones 2−5 obey the following condition assuming that the void fractions (ε_I and ε_P) of the columns in the upper and lower layers are the same

$$r_V = \frac{d_L}{d_U} = \frac{m_{3U} - m_2}{m_2 - m_{3L}} = \frac{m_{4U} - m_5}{m_5 - m_{4L}} \tag{6}$$

where r_V is the volume ratio of the lower layer to the upper layer, d_L is the distance between operating points (m_{3U}, m_{4U}) and (m_2, m_5), and d_U is the distance between operating points (m_{3L}, m_{4L}) and (m_2, m_5), cf. Figure 2. This means that five m-values can determine the operating conditions of zones 2−5, i.e., three operating points (m_{3U}, m_{4U}), (m_{3L}, m_{4L}), and (m_2, m_5) are on a straight line. By determining the operating conditions, the volume ratio is also determined. However, the dimensions of the upper- and lower-layer columns, which affect the zone pressure drop and column efficiencies, should be considered as a design parameter.

If the port switching interval is fixed, seven m-values can determine the operating conditions. In this work, the m-value of zone 5, m_5, was determined from eq 6. The volumetric flow rates in each zone can be obtained as below

$$Q_{jU} = \frac{V_{C,U}\{\varepsilon_T + (1 - \varepsilon_T)m_{jU}\}}{t_S} \tag{7.1}$$

$$Q_{jL} = \frac{V_{C,L}\{\varepsilon_T + (1 - \varepsilon_T)m_{jL}\}}{t_S} \tag{7.2}$$

For the paired double-layer zones in which both layers have the same role, the m-values are the same, e.g., $m_1 = m_{1U} = m_{1L}$.

2.2. Hybrid Double-Layer SMB: Serial Column Connections in Paired Double-Layer Zones. It is straightforward to simplify the internal flow patterns by serializing the column connections in the paired double-layer zones so that each column pair can be connected in series and no flow split unit is required. Figure 3 shows the upper-to-lower (UL) serial connection of the paired double-layer zone. Since the location of the first column pair is moved at the last position of the precedent zone for the next periodic operation, the serial connection should be made in pair-to-pair.

The art of intermediate-retained component separation arises from parallelization of the layers in the divided double-layer zones (zones 3 and 4) so that it is worth keeping them in parallel.

https://doi.org/10.1021/acs.iecr.1c01268
Ind. Eng. Chem. Res. 2021, 60, 8911−8926

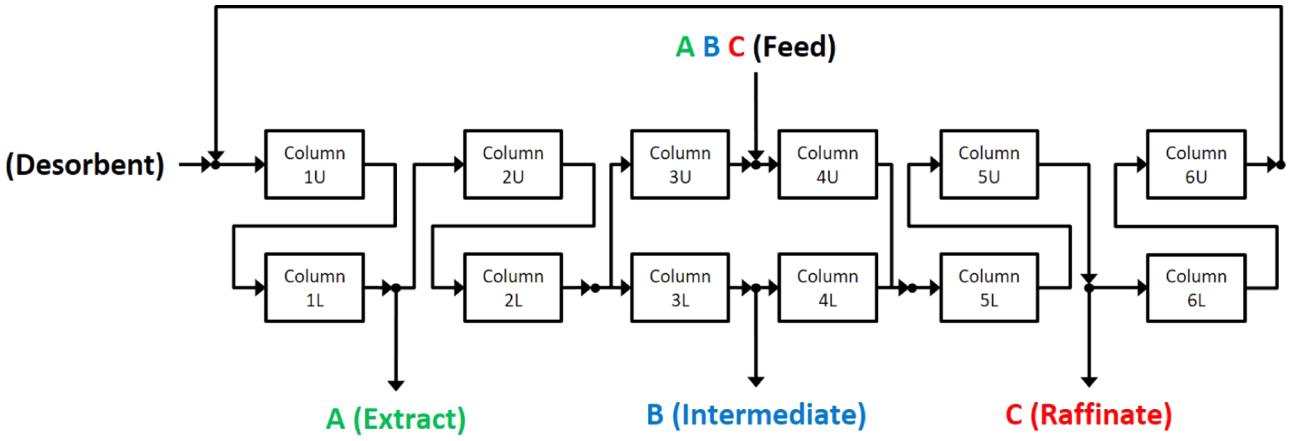

Figure 4. Flow diagram of the hybrid double-layer SMB with the 12-column configuration. Zones 1 and 2: upper-to-lower (UL) serial connection; zones 5 and 6: lower-to-upper (LU) serial connection.

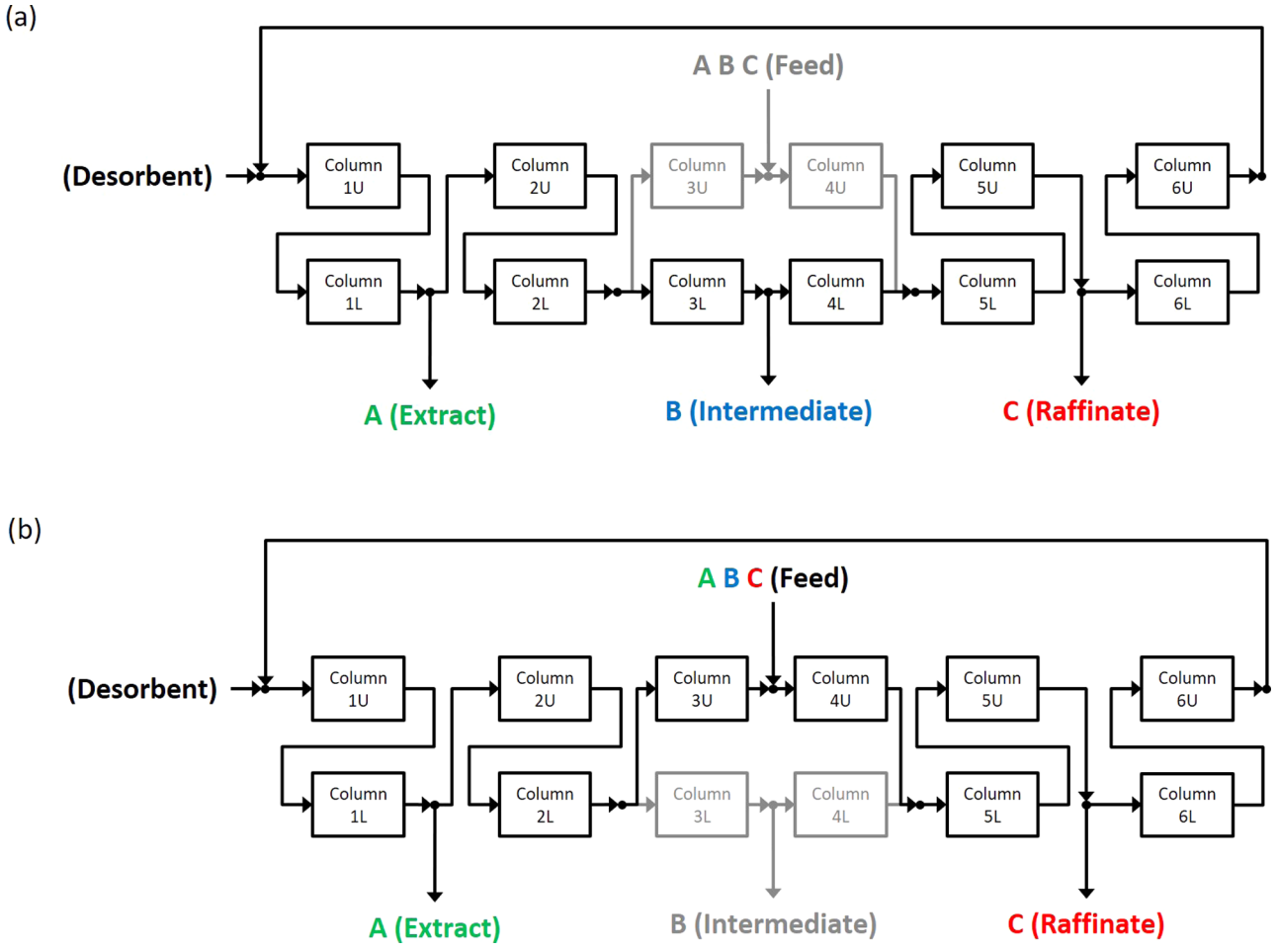

Figure 5. Flow diagram of the serial double-layer SMB with the step-by-step operation of the divided double-layer zones. (a) Step operation for the intermediate port and (b) step operation for the feed port. Gray blocks and streams indicate no flow; LU (in zones 1 and 2) and UL (in zones 5 and 6) serial connection.

This hybrid double-layer SMB configuration was considered as one alternative layer configuration. One design parameter, the mode of serial column connections, should be determined to design the hybrid double-layer SMB. Figure 4 shows one possible flow diagram of the hybrid double-layer SMB with 12 columns. The upper-to-lower (UL) serial connections and the lower-to upper (LU) serial connections were applied in zones 1 and 2 and in zones 5 and 6, respectively. Since the hybrid double-layer SMB requires one flow split unit at the inlet of zone 3, the volumetric flow rates in the divided double-layer zones can be obtained by eqs 7.1 and 7.2. For the paired double-layer zones, the zone flow rate is the summation of the flow rates of the upper and lower layers

https://doi.org/10.1021/acs.iecr.1c01268
Ind. Eng. Chem. Res. 2021, 60, 8911−8926

$$Q_j = Q_{jU} + Q_{jL} = \frac{(V_{C,U} + V_{C,L})\{\varepsilon_T + (1 - \varepsilon_T)m_j\}}{t_S} \quad (8)$$

It was assumed that the column properties, the void fractions, and the particle properties are the same in both layers.

2.3. Serial Double-Layer SMB: Discrete Step Operation in Divided Double-Layer Zones. In liquid chromatography, the system void volumes that may affect the significant loss of separation performances result from the fittings, tubings, and peripherals out of the columns. Especially, a flow split unit that uses a chromatographic pump causes a sizable system void volume compared to a flow selection valve. Note that the operation of SMB is periodically repeated at intervals of port switching, and many variations of multistep flow changes can be made in one port switching interval by maintaining the same average flow rate ratios.[2−5] Adapting one advanced flow modulation concept, the flow-focusing operation,[5] it was possible to operate the upper and lower layers consecutively; the intermediate port opened with focused flow rate (higher than normal operation); meanwhile, the upper zone flow rates (Q_{3U} and Q_{4U}) were zero (no feed flow) and vice versa (cf. Figure 5a,b, respectively).

The switches of the zone 2 outlet and the zone 5 inlet were synchronized, and these flow rates were correspondingly changed by the step operation of the divided double-layer zones. However, the average zone flow rates should be the same as the zone flow rates of the corresponding parallel operation to maintain the roles of the zones mentioned above, i.e., the total elution volumes of the corresponding zones should be the same for one port switching interval. To design this operation mode, two design parameters, the ratio of the focused flow interval and the position of the focused flow, need to be determined. The zone flow rates in two distinct steps can be obtained as below:

Feed flow-focusing step

$$Q_1^{FF} = \frac{V_{C,U}\{\varepsilon_T + (1 - \varepsilon_T)m_1\}}{r_{FF}t_S} \quad (9)$$

$$Q_2^{FF} = Q_{3U}^{FF} = \frac{V_{C,U}\{\varepsilon_T + (1 - \varepsilon_T)m_{3U}\}}{r_{FF}t_S} \quad (10)$$

$$Q_5^{FF} = Q_{4U}^{FF} = \frac{V_{C,U}\{\varepsilon_T + (1 - \varepsilon_T)m_{4U}\}}{r_{FF}t_S} \quad (11)$$

$$Q_{3L}^{FF} = Q_{4L}^{FF} = 0 \quad (12)$$

$$Q_6^{FF} = \frac{V_{C,U}\{\varepsilon_T + (1 - \varepsilon_T)m_6\}}{r_{FF}t_S} \quad (13)$$

Intermediate flow-focusing step

$$Q_1^{IF} = \frac{V_{C,L}\{\varepsilon_T + (1 - \varepsilon_T)m_1\}}{r_{IF}t_S} \quad (14)$$

$$Q_{3U}^{IF} = Q_{4U}^{IF} = 0 \quad (15)$$

$$Q_2^{IF} = Q_{3L}^{IF} = \frac{V_{C,L}\{\varepsilon_T + (1 - \varepsilon_T)m_{3L}\}}{r_{IF}t_S} \quad (16)$$

$$Q_5^{IF} = Q_{4L}^{IF} = \frac{V_{C,L}\{\varepsilon_T + (1 - \varepsilon_T)m_{4L}\}}{r_{IF}t_S} \quad (17)$$

$$Q_6^{IF} = \frac{V_{C,L}\{\varepsilon_T + (1 - \varepsilon_T)m_6\}}{r_{IF}t_S} \quad (18)$$

where r_{FF} and r_{IF} are the ratios of the flow-focusing step in one port switching interval for the feed flow and the intermediate flow, respectively ($0 < r < 1$; $r_{FF} + r_{IF} = 1$). Since the operation steps are composed in one port switching interval, two alternative step operations were considered. In the "serial-1" step operation, the feed flow-focusing step was located in the middle, and the step order was

- Step 1: Intermediate flow focusing with eqs 14−18 for $s_{FF}(1 - r_{FF})t_S$.
- Step 2: Feed flow focusing with eqs 9−13 for $r_{FF}t_S$.
- Step 3: Intermediate flow focusing with eqs 14−18 for $(1 - s_{FF})(1 - r_{FF})t_S$.

In "serial-2" step operation, the intermediate flow-focusing step was located in the middle, and the step order was

- Step 1: Feed flow focusing with eqs 9−13 for $s_{IF}(1 - r_{IF})t_S$.
- Step 2: Intermediate flow focusing with eqs 14−18 for $r_{IF}t_S$.
- Step 3: Feed flow focusing with eqs 9−13 for $(1 - s_{IF})(1 - r_{IF})t_S$.

where s_{FF} and s_{IF} are the positions of the feed and intermediate flow-focusing steps ($0 \le s_{FF} \le 1$; $0 \le s_{IF} \le 1$), respectively. Since serial-1 and serial-2 operations utilized the same operation steps, the serial-1 and serial-2 operations were identical if $s_{FF} = 0$ and $s_{IF} = 1$ (or $s_{FF} = 1$, and $s_{IF} = 0$) and $r_{FF} = 1 - r_{IF}$.

2.4. Pressure Drop of Double-Layer SMBs. The pressure drop of the chromatographic column is proportional to the linear velocity of the mobile phase and the column length. Even though the column volume and the volumetric flow rate of the mobile phase are the same, the pressure drop varies by the dimensions of the column. The mobile-phase flow rate is laminar flow in general liquid chromatographic conditions. Therefore, the pressure drop of the chromatographic column was calculated by the Kozeny equation.[10] Assuming that the column and mobile-phase properties (void fraction, viscosity, and particle diameter) are constant, the pressure drop is directly proportional to the volumetric flow rate of the mobile phase and the length of the column but inversely proportional to the square of the column diameter.

$$\Delta P_{j,k} = \frac{150\mu_L}{D_p^2}\frac{(1 - \varepsilon_I)^2}{\varepsilon_I^3}\frac{Q_j L_{C,k}}{(\pi/4)D_{C,k}^2} \quad (19)$$

where ΔP is the pressure drop, μ_L is the viscosity of the mobile phase, D_p is the particle diameter, L_C is the column length, D_C is the column diameter, and the subscripts j and k denote zone j and column k, respectively.

In the parallel double-layer SMB, the pressure drop of the paired double-layer zone was determined in conformity with the layer that generates a higher pressure drop. The pressure drop of the paired double-layer zone is

$$\Delta P_j = \max\begin{pmatrix}\Delta P_{jU}\\ \Delta P_{jL}\end{pmatrix} = \max\begin{pmatrix}\sum_k \Delta P_{jU,k}\\ \sum_k \Delta P_{jL,k}\end{pmatrix} \quad (20)$$

where subscript j denotes the pared double-layer zones. The upper and lower layers generate uniform pressure drops if the lengths and the m-values of both layers are the same. In the

https://doi.org/10.1021/acs.iecr.1c01268
Ind. Eng. Chem. Res. 2021, 60, 8911−8926

hybrid and serial double-layer SMB, the pressure drop of the paired double-layer zone was determined by the summation of both layer pressure drops because of the serial column connection. The pressure drop of the paired double-layer zone with serial connection is

$$\Delta P_j = \Delta P_{j\mathrm{U}} + \Delta P_{j\mathrm{L}} = \sum_k \Delta k P_{j\mathrm{U},k} + \sum_k \Delta P_{j\mathrm{L},k} \tag{21}$$

To minimize the zone pressure drop in the fixed layer volume ratio, the upper- and lower-layer columns should have the same diameter.

In the divided double-layer zones of the parallel and hybrid double-layer SMBs, the split zone 3 inlet flows merged at the zone 4 outlet so that the pressure drops of zones 3 and 4 were determined in conformity with the layer that generates a higher pressure drop. The pressure drop of the divided double-layer zone, $\Delta P_3 + \Delta P_4$, can be obtained from eq 20. In the serial double-layer SMB that adapts the flow-focusing operation concept, the flow rates of the upper-layer columns were zero during the lower-layer columns were operated in zones 3 and 4 and vice versa. Therefore, the pressure drops of zones 3 and 4, $\Delta P_3^{\mathrm{FF}} + \Delta P_4^{\mathrm{FF}}$ or $\Delta P_3^{\mathrm{IF}} + \Delta P_4^{\mathrm{IF}}$, can be obtained from eq 21.

The pressure drop of the SMB system depends on the configuration of the pumps and columns. If the pumps are located at the inlet of the zone to control the zone flow rates directly, the system pressure drop is determined by the zone that generates the highest pressure drop. However, this configuration includes large system void volumes in the SMB ring. In this work, other configurations, in which one recycle stream, all external stream, and one of the layer stream flow rates were controlled by the pumps, was considered to minimize the system void volumes in the SMB ring (cf. Table 5). Therefore, the system pressure drop was the summation of the pressure drops from zone 1 to zone 6

$$\Delta P_{\mathrm{SMB}} = \sum_{j=1}^{6} \Delta P_j \tag{22.1}$$

where ΔP_{SMB} is the pressure drop of the SMB system. In the serial double-layer SMB, each operation step was operated with different zone flow rates and the upper and lower layers were intermittently operated. Therefore, the pressure drop of the SMB system was determined by the operation step that caused a higher pressure drop.

$$\Delta P_{\mathrm{SMB}} = \max\left(\sum_{j=1}^{6} \Delta P_j^{\mathrm{FF}}, \sum_{j=1}^{6} \Delta P_j^{\mathrm{IF}}\right) \tag{22.2}$$

3. PROCESS DESCRIPTION AND DETAILED SIMULATION STUDY

3.1. Process Model. To investigate the layer configurations introduced in Section 2, a detailed simulation study was conducted assuming that the SMB processes are ideal (identical column properties and no system void volume). The same ternary separation problems discussed in the previous work[8] were chosen. A chromatographic column model that includes the mass balance, linear driving force mass transfer, and linear isotherms was considered.

$$\varepsilon_{\mathrm{T}} \frac{\partial c_i}{\partial t} + (1 - \varepsilon_{\mathrm{T}}) \frac{\partial q_i}{\partial t} + v_{\mathrm{L}} \frac{\partial c_i}{\partial z} = \varepsilon_{\mathrm{I}} D_{\mathrm{L}} \frac{\partial^2 c_i}{\partial z^2} \tag{23}$$

$$\frac{\partial q_i}{\partial t} = k_{\mathrm{eff},i}(q_i^* - q_i) \tag{24}$$

$$q_i^* = K_i c_i \tag{25}$$

where c and q are respectively the concentrations in the mobile and the stationary phases, q^* is the equilibrium concentration of the solid film, D_{L} is the axial dispersion coefficient, k_{eff} is the mass-transfer coefficient, v_{L} is the linear velocity of the mobile phase, and subscript i denotes component i. The model parameters are listed in Table 1. The mass-transfer coefficient k_{eff} determines the mass-transfer rate in the solid film so that the elution band is more broadened as k_{eff} decreases, i.e., the mass-transfer resistance increases. The double-layer SMB requires at least 12 columns to compose 12 zones. The simplest column configuration, one column per zone configuration was considered. To decide the dimensions of the column, the

Table 1. Parameters and Operating Conditions for the Detailed Simulation Study of the Double-Layer SMB[8,11−13]

parameters	values
process	
column configuration	one column per zone
upper-layer column diameter, $D_{\mathrm{C,U}}$ (cm)	1.0
length of one column pair, $L_{\mathrm{C,T}}$ (cm)	30
column void fraction, ε_{I} and ε_{P}	0.4, 0.667
port switching interval, t_{S} (min)	10 (for the design parameter screening)
particle diameter, D_{P} (μm)	30
viscosity of the mobile phase, μ_{L} (cP)	0.797[a]
model mixture (dA, dT, dG, dC)	
isotherm model	linear
isotherm parameters, K_i in eq 25	27.7, 9.6, 7.4, 3.15
mass-transfer coefficient, $k_{\mathrm{eff},i}$ in eq 24 (min^{-1})	6.0, 30, 30, 60
axial dispersion coefficient, D_{L} in eq 23 (cm^2/min)	0.225
feed concentration, dA/dT/dG (g/L)	1.0/1.0/1.0
feed concentration, dT/dG/dC (g/L)	1.0/1.0/1.0
simulation[b]	
PDE solver	FVM with OSPRE scheme
spatial nodes (nodes/cm)	8
# of port switching interval	91
operating conditions[c]	
separation case 1: dA/dT/dG	33.2/24.4/8.14/24.9/24.9/8.14/5.92
separation case 2: dA/dT/dG	33.2/10.6/8.14/24.9/10.6/8.14/5.92
separation case 3: dT/dG/dC	11.5/8.14/3.47/8.64/8.64/3.47/2.52
separation case 4: dT/dG/dC	11.5/8.14/3.47/8.64/8.64/6.47/2.52

[a]Viscosity of pure water at 30 °C. [b]Aspen Chromatography (Aspen Tech Inc., ver. 8.8). [c]$m_1/m_2/m_{3\mathrm{U}}/m_{4\mathrm{U}}/m_{3\mathrm{L}}/m_{4\mathrm{L}}/m_6$; $m_5 = (m_{4\mathrm{U}} + r_{\mathrm{V}} m_{4\mathrm{L}})/(1 - r_{\mathrm{V}})$.

https://doi.org/10.1021/acs.iecr.1c01268
Ind. Eng. Chem. Res. 2021, 60, 8911−8926

Table 2. Range of the Orthogonal Parameter Screening of the Design Parameters

	column length in the upper layer, $L_{C,U}$ (cm)	serial column connection	ratio of flow focusing, r_{FF} or r_{IF}	position of flow focusing, s_{FF} or s_{IF}
parallel	$L_{C,U,Min}$ ~ 27.5 (2.5 intv.)	N/A	N/A	N/A
hybrid	$L_{C,U,Min}$ ~ 15 (2.5 intv.)	(UL/LU)−(UL/LU)	N/A	N/A
serial-1	$L_{C,U,Min}$ ~ 15 (2.5 intv.)	(UL/LU)−(UL/LU)	0.1−0.5 (0.1 intv.)	0−1 (0.25 intv.)
serial-2	$L_{C,U,Min}$ ~ 15 (2.5 intv.)	(UL/LU)−(UL/LU)	0.5−0.9 (0.1 intv.)	0−1 (0.25 intv.)
standard[a]	15	UL−LU	0.5	0.5

[a]The standard values for the design parameter screening.

column diameter of the upper layer was fixed to 1 cm and the length of one column pair was fixed to 30 cm. According to the column length in the upper layer, the dimensions of the column in the lower-layer were determined by eq 6.

For the separation of each model mixture (dA/dT/dG and dT/dG/dC), two operating conditions were determined with the same safety margins (10% for the separation regions and 20% for the regeneration region) as the previous work.[8] For complete regeneration of the adsorbent and desorbent, the safety margins for the regeneration zones were set higher so that the desorbent consumption and the enrichment of raffinate and extract product could be improved further optimization of m_1 and m_6. Design parameters m_2 and m_{3L} can be chosen in a certain range if the Henry constant difference of the most- and intermediate-retained components is greater than that of the intermediate- and least-retained components. In the opposite case, m_{4L} and m_5 can be chosen in a certain range. Therefore, two extreme operating conditions were chosen by maintaining constant r_V; they provide theoretically the same product purity but different product enrichments.[8] The operating points on the m-value plane are drawn in Figure 2.

A commercial chromatographic process simulator, Aspen Chromatography (Aspen Tech Inc., ver. 8.8), was used. To obtain the process simulation results in the cyclic steady state, the simulations were carried out for up to 91 port switching intervals (15 complete SMB cycles and 1 cycle for the observation of the internal profiles).

3.2. Orthogonal Parameter Screening to Determine the Design Parameters. Assuming that the design parameters are orthogonal, the design parameters could be individually screened to determine the optimal design. The design parameters were screened, as shown in Table 2. The dimensions of the columns in both layers should be determined according to the column volume ratio obtained from the m-values, cf. the operating conditions in Table 1. The length of one column pair ($L_{C,T}$) and the diameter of the upper-layer column ($D_{C,U}$) were fixed. Therefore, the dimensions of the columns could be calculated from the length of the upper-layer column

$$D_{C,L} = \sqrt{\frac{r_V L_{C,U}}{L_{C,T} - L_{C,U}}} D_{C,U} \text{ s. t. } L_{C,T} = L_{C,U} + L_{C,L} \tag{26}$$

where $L_{C,T}$ is the total column length. In every separation case, the volume of the upper layer was smaller than the volume of the lower layer ($r_V > 1$) so that it was preferable to set smaller the diameter of the upper-layer column than the diameter of the lower-layer column. Therefore, the length of the upper-layer column is minimized where the column diameters are the same in both layers,

$$L_{C,U,Min} = \frac{L_{C,T}}{1 + r_V} \tag{27}$$

where $L_{C,U,Min}$ is the minimum length of the upper-layer column. The length of the upper-layer column was screened from $L_{C,U,Min}$ at intervals of 2.5 cm. In the parallel double-layer SMB, the pressure drop of the paired double-layer zone was determined by one dominant layer that causes a higher pressure drop, cf. eq 20. Therefore, the entire range of $L_{C,U}$ was screened (up to 27.5 cm). However, the pressure drop of the paired double-layer zone with serial column connection increased as the length of the upper-layer column increased because the fast linear velocity of the mobile phase is imposed due to the small diameter of the upper-layer column. The column length was screened up to 15 cm for the hybrid and serial double-layer SMBs.

The column pairs in the paired double-layer zones could be serialized either the upper-to-lower (UL) or the lower-to-upper (LU) connections. Since the positions of columns were switched pair-to-pair, it was preferred to have the same serialized connection in neighbored zones, i.e., the serial connections of zones 1 and 2 and zones 5 and 6 are the same. Four serial connection types (UL or LU in zones 1 and 2) × (UL or LU in zones 5 and 6) were screened.

In the serial double-layer SMB, there are two alternative step-operation variations (serial-1, centered feed flow focusing; serial-2, centered intermediate flow focusing), and two design parameters, the ratio and position of the flow focusing step, need to be determined. The upper-layer volume was smaller than the lower-layer volume so that the feed stream flow rate was smaller than the intermediate stream flow rate. Since the pressure drop of the SMB system became higher as the intermediate stream was focused in a narrower operation step (smaller r_{IF} or bigger r_{FF}), the r_{FF} was screened from 0.1 to 0.5 and the r_{IF} was screened from 0.5 to 0.9. The position of the flow-focusing step, s_{FF} or s_{IF}, did not affect the system pressure drop but the product quality so that they were screened from 0 to 1 at intervals of 0.25. The standard design parameters were chosen as 15 cm of $L_{C,U}$, UL−LU serial connection of the paired double-layer zones, 0.5 of the flow-focusing ratio, and 0.5 of the flow-focusing position. When a chosen design parameter was screened, other design parameters were fixed to the standard design parameters.

To decide the optimal design parameters from the screened results, the averaged purity and yield and the system pressure drop, cf. eqs 22.1 and 22.2, were considered. In the cyclic steady state, the averaged purity $\overline{\text{Pur}}$ and yield $\overline{\text{Yld}}$ were obtained as

$$\overline{\text{Pur}} = \frac{\sum_m \text{Pur}_m}{\#M} \text{ s. t. } \text{Pur}_m = \frac{\int_{t=t_{CSS}}^{t_{CSS}+t_S} c_{l,m} Q_m}{\sum_i \int_{t=t_{CSS}}^{t_{CSS}+t_S} c_{i,m} Q_m} \times 100 \tag{28}$$

https://doi.org/10.1021/acs.iecr.1c01268
Ind. Eng. Chem. Res. 2021, 60, 8911−8926

Table 3. Comparisons of Various Layer Configurations of Double-Layer SMB in Terms of the Averaged Process Performances and the System Pressure Drop with the Standard Design Parameters

sep. case	$L_{C,U}$ (cm)	layer config.[a]	$r_{FF}(r_{IF})/s_{FF}(s_{IF})$	t_S (min)	$\overline{Pur}$ (%)	$\overline{Yld}$ (%)	$\overline{Pr} \times 10^3$ (g/(L h))	$\overline{DC}$ (L/g)	ΔP_{SMB} (bar)	$F_{Obj} \times 10^3$
1	15	P-P-P	N/A	10	96.0	95.4	92.6	60.2	7.24	0..0213
	15	UL-P-LU	N/A	10	98.1	97.8	95.0	58.5	178	0.567
	15	UL-S1-LU	0.5/0.5	10	95.8	95.5	92.7	60.0	346	0.0223
	15	UL-S2-LU	0.5/0.5	10	94.2	93.7	91.0	61.1	346	0.0
2	15	P-P-P	N/A	10	99.5	99.5	96.4	57.6	6.46	1.34
	15	UL-P-LU	N/A	10	99.0	99.0	95.9	57.9	151	1.06
	15	UL-S1-LU	0.5/0.5	10	97.7	97.7	94.7	58.7	291	0.470
	15	UL-S2-LU	0.5/0.5	10	97.3	97.3	94.3	58.9	291	0.335
3	15	P-P-P	N/A	10	97.9	97.7	122	19.5	3.49	1.99
	15	UL-P-LU	N/A	10	97.4	97.3	121	19.5	28.2	1.38
	15	UL-S1-LU	0.5/0.5	10	97.6	97.6	122	19.5	51.1	1.73
	15	UL-S2-LU	0.5/0.5	10	96.7	96.5	121	19.7	51.1	0.655
4	15	P-P-P	N/A	10	99.3	99.3	124	19.1	3.81	4.81
	15	UL-P-LU	N/A	10	98.6	98.5	123	19.3	30.1	3.20
	15	UL-S1-LU	0.5/0.5	10	97.2	97.2	121	19.6	54.6	1.18
	15	UL-S2-LU	0.5/0.5	10	97.3	97.0	121	19.6	54.6	1.16

[a]{Zones 1 and 2}-{zones 3 and 4}-{zones 5 and 6}; P, parallel; S1, serial-1; S2, serial-2; UL, upper-to-lower; LU, lower-to-upper.

$$\overline{Yld} = \frac{\sum_m Pur_m}{\#M} \text{ s. t. } Yld_m = \frac{\int_{t=t_{CSS}}^{t_{CSS}+t_S} c_{l,m} Q_m}{\int_{t=t_{CSS}}^{t_{CSS}+t_S} c_{l,Feed} Q_{Feed}} \times 100 \quad (29)$$

where t_{CSS} is the operation time until the process reaches cyclic steady state ($=90t_S$), M is the set of the product streams, subscript m denotes the product stream, and subscript l denotes the product component corresponding to the product stream m. The product streams are the extract (Extr), intermediate (Intm), and raffinate (Raff) for the more-, intermediate-, and less-retained components, respectively.

3.3. Screening of Port Switching Interval. Since the m-values of the regeneration zones (zones 1 and 6) were decided with relatively large safety margins to accomplish complete regeneration of the mobile and stationary phases, i.e., product contamination through the recycle stream between zones 1 and 6 is negligible, the extract and raffinate products are produced with high purity and yield if the purity and yield of the intermediate product are high enough. This means that the performances of the double-layer SMB increase as the separation capacity of the column increases with high column efficiency. When a short port switching interval is applied, the feed throughput increases, but the column efficiency, which may affect desorbent consumption, is worse due to the limited mass-transfer rate. Therefore, two more process performances, productivity and desorbent consumption, were considered to optimize the port switching interval. In the cyclic steady state, the averaged productivity $\overline{Pr}$ and desorbent consumption $\overline{DC}$ were obtained as

$$\overline{Pr} = \frac{\sum_m Pr_m}{\#M} \text{ s. t. } Pr_m = \frac{\int_{t=t_{CSS}}^{t_{CSS}+t_S} c_{l,m} Q_m}{6\varepsilon_T t_S (V_{C,U} + V_{C,U})} \quad (30)$$

$$\overline{DC} = \frac{\sum_m DC_m}{\#M} \text{ s. t. } DC_m = \frac{\int_{t=t_{CSS}}^{t_{CSS}+t_S} Q_{Feed} + \int_{t=t_{CSS}}^{t_{CSS}+t_S} Q_{Dsrb}}{\int_{t=t_{CSS}}^{t_{CSS}+t_S} c_{l,m} Q_m} \quad (31)$$

where subscripts Feed and D_{srb} denote the feed and desorbent streams, respectively. Using an objective function as below, the optimal port switching interval was determined where the objective function was maximized.

$$F_{Obj} = w_{Pur} w_{Yld} \left(\frac{\overline{Pr}}{\overline{DC}} \right) \quad (32.1)$$

$$w_{Pur} = \max\left\{ \frac{\overline{Pur} - \widehat{Pur}}{100 - \widehat{Pur}}, 0 \right\} \quad (32.2)$$

$$w_{Yld} = \max\left\{ \frac{\overline{Yld} - \widehat{Yld}}{100 - \widehat{Yld}}, 0 \right\} \quad (32.3)$$

where w_{Pur} and w_{Yld} are respectively the weighting factors regarding two design constraints, purity and yield, and $\widehat{Pur}$ and $\widehat{Yld}$ are the minimum purity and yield constraints, respectively. The objective function has a nonzero weighting factor value if and only if the averaged purity and yield satisfy the minimum purity and yield constraints. The minimum purity and yield constraints were set to 95%. The third term $\overline{Pr}/\overline{DC}$ represents the process economy; as the productivity increases and the desorbent consumption decreases, the process economy increases. The port switching interval was screened at intervals of 10 min and then finely screened at intervals of 2 min. From this screening, the port switching intervals that provide the highest product quality, $GM(\overline{Pur}, \overline{Yld}) = \sqrt{\overline{Pur} \cdot \overline{Yld}}$ and maximize the objective function values were determined by the natural cubic spline interpolation.[14]

To compare the process complexity of various layer configurations of the double-layer SMB introduced in this work and two alternative ternary SMBs discussed in the previous work,[8] the structural and operational complexities were applied[15]

$$I_{SC} = w_C N_C + w_V N_V + w_P N_P + w_T N_T \quad (33)$$

$$I_{OC} = w_O N_O + w_R N_R \quad (34)$$

where I_{SC} and I_{SC} are respectively the index of structural complexity and the index of operational complexity; N_C, N_V, N_P,

https://doi.org/10.1021/acs.iecr.1c01268
Ind. Eng. Chem. Res. 2021, 60, 8911−8926

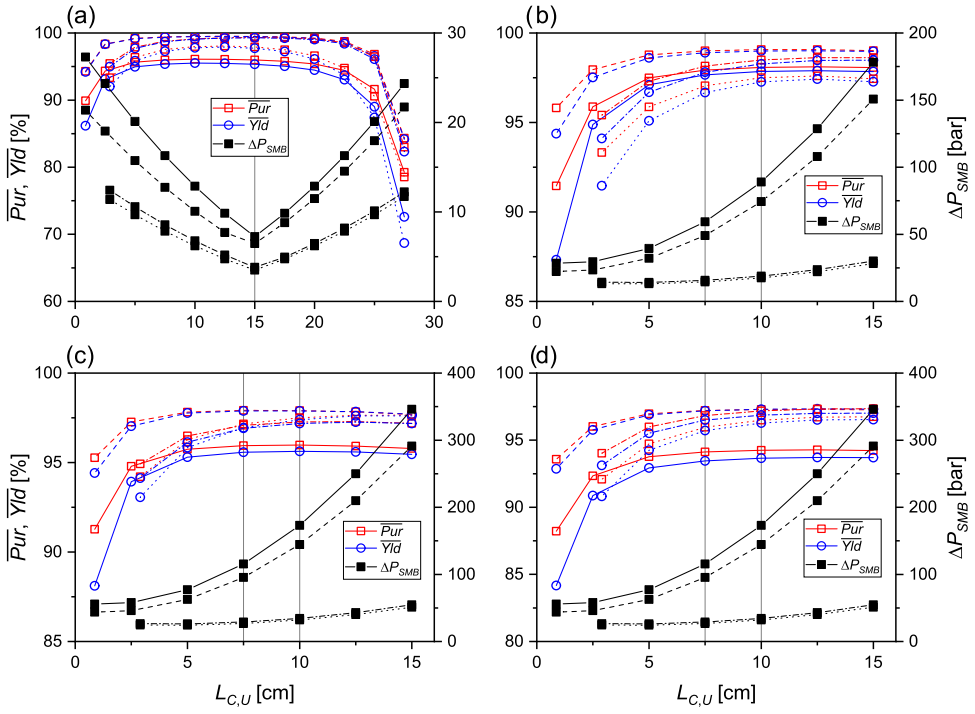

Figure 6. Screening of the length of the upper-layer column in terms of the average purity and yield and the pressure drop of the SMB system. (a) Parallel layer configuration, (b) hybrid layer configuration, (c) serial-1 layer configuration, and (d) serial-2 layer configuration. Solid line, separation case 1; dashed line, separation case 2; dotted line, separation case 3; dash-dot line, separation case 4; and vertical gray lines, chosen optimal column lengths. Other design parameters were fixed to the standard values in Table 2.

N_T, N_O, and N_R are respectively the number of columns, valves, pumps, tanks, operations, and recycles; and w_C, w_V, w_P, w_T, w_O, and w_R are the corresponding weighting factors. All weighting factors are arbitrary fixed to 1.0. All valves are assumed to be on−off valves. The number of operations in the SMB process is the number of operating conditions applied in the columns during one port switching interval. For example, the conventional four-zone four-column SMB requires at least 4 columns, 16 on−off valves (4 valves at each column outlet), four pumps, and no tank. Each zone is operated with different flow rates for one port switching interval. The connection of columns forms a ring so that it has one recycle stream. Therefore, the index of structural complexity is 24 and the index of operational complexity is 5, where all weighting factors are 1.0.

4. RESULTS AND DISCUSSION

The design parameters—the length of the upper-layer column, the column connection of the paired double-layer zones, the ratio of the flow-focusing step, and the position of the flow-focusing step—were screened on the basis of the standard design parameters. Table 3 compares four different types of layer configurations with the standard design parameters. Since the same operating conditions are applied in each separation case, the feed and solvent throughputs are all the same. Therefore, the averaged productivity and desorbent consumption were similar.

In separation case 1, the hybrid double-layer SMB (UL-P-LU layer configurations) provides better process performances than other layer configurations. The serial column connections in the paired double-layer zones may have the advantage. It will be discussed later. In other separation cases, the parallel double-layer SMB (P-P-P) provides better process performances than other layer configurations.

In the parallel double-layer SMB, all zones are operated in parallel with complex internal flow patterns. This means that a low flow rate is applied in a small volume column and vice versa. Therefore, the parallel double-layer SMB generates the smallest system pressure drops for all separation cases. As the layers are serialized, i.e., the columns are connected in series and the layer operations are intermittently carried out with focused high flow rate, the system pressure drops increase. In separation cases 1 and 2 (r_V = 33.5), the hybrid double-layer SMB and the serial double-layer SMB generate approx. 24 times and 46 times higher pressure drop than the parallel double-layer SMB, respectively. In separation cases 3 and 4 (r_V = 9.4), the hybrid and serial double-layer SMBs generate less increased system pressure drops (8 times and 14 times higher, respectively) compared to the separation cases 1 and 2. If the volume ratio increases, the difference of the diameters of the upper- and lower-layer columns increases and it causes high pressure drops in the serialized column connections. Since the zone flow rates are focused on the serial double-layer SMBs, the system pressure drops are much higher than the hybrid double-layer SMB. Therefore, it is required that the design parameters should be optimized to generate low system pressure drops while maintaining the process performances.

The objective function value, which represents the process economy, of the double-layer SMB with serial-2 layer configuration was zero because the averaged purity and yield could not satisfy the minimum constraints, $\widehat{Pur}$ = 95% and $\widehat{Yld}$ = 95%. For separation case 1, the hybrid double-layer SMB provides a much higher process economy because of high product quality. However, the parallel double-layer SMB provides the highest process economy for all other separation cases. These comparisons were done with the standard design parameters.

https://doi.org/10.1021/acs.iecr.1c01268
Ind. Eng. Chem. Res. 2021, 60, 8911−8926

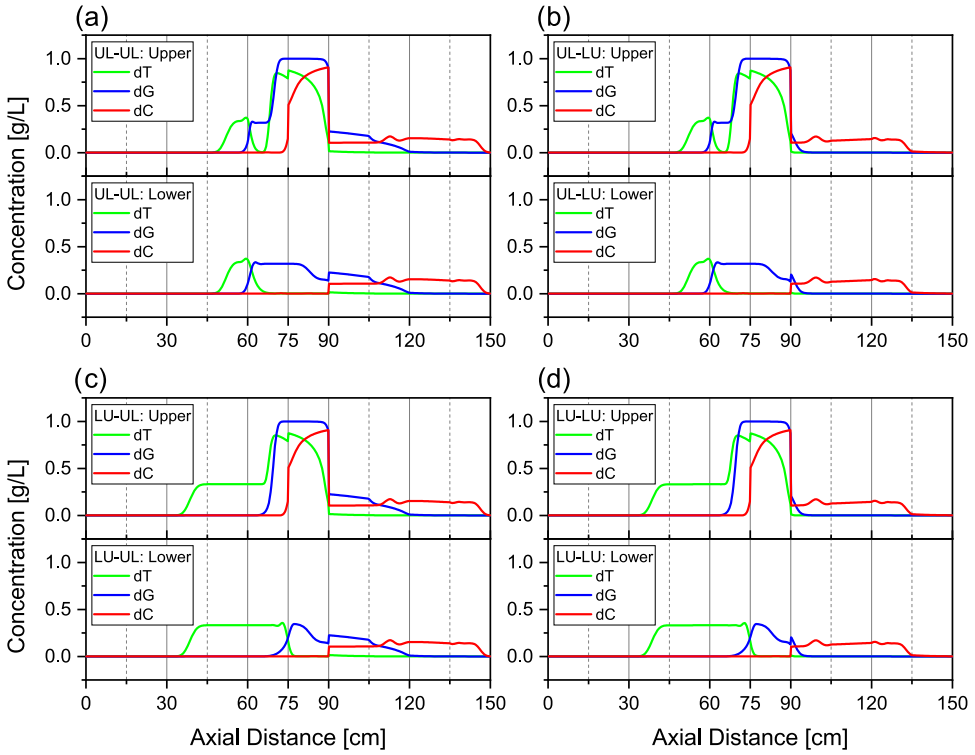

Figure 7. Comparisons of the internal concentration profiles of the hybrid double-layer SMBs for separation case 4 with various serial connections of paired double-layer zones at the end of the port switching interval of cyclic steady state. (a) UL in zones 1 and 2 and UL in zones 5 and 6 (UL−UL), (b) UL in zones 1 and 2 and LU in zones 5 and 6 (UL−LU), (c) LU in zones 1 and 2 and UL in zones 5 and 6 (LU−UL), and (d) LU in zones 1 and 2 and LU in zones 5 and 6 (LU−LU). 0−60 cm, serialized columns in zones 1 and 2; 60−90 cm, upper and lower columns in zones 3 and 4; 90−150 cm, serialized columns in zones 5 and 6; solid vertical gray lines, zone boundaries; dashed vertical gray lines, column boundaries. Other design parameters were fixed to the standard values in Table 2.

Since up to four design parameters were needed to be screened (cf. Table 2), it was assumed that all design parameters are orthogonal, i.e., the set of the optimal design parameters that are individually determined by the single variable screening is also optimal set, to avoid "curse of dimensionality".

4.1. Screening of Upper-Layer Column Length. In the double-layer SMB, the volume ratio of the lower- to upper-layer columns is determined by the *m*-values, cf. eq 6. The pressure drop of the column is proportional to the length of the column and the linear velocity of the mobile phase, eq 19. The process model applied in this work does not contain any radial dispersion effect but the axial dispersion and limited mass-transfer rate so that the length of the column and the linear velocity of the mobile phase also affect the column efficiency. Therefore, the dimensions of the upper- and lower-layer columns are critical to the performance of the process.

Figure 6 shows the changes in average purity and yield and the system pressure drop by the length of the upper-layer column. Where the lengths of the upper- and lower-layer columns were the same as 15 cm in the parallel double-layer SMB (Figure 6a), the pressure drops of the upper- and lower-layer columns were the same and the system pressure drop was minimized. If the length of the upper-layer column is too short or too long, two columns that have quite different efficiencies are paired as a single column in the paired double-layer zones. It causes bad separation capacity by "loss of efficiency". In divided double-layer zones, the main roles of both layers are to isolate the intermediate-retained component so that the intermediate product stream can be contaminated if the efficiency of any column in the divided double-layer zones is not sufficiently high. The averaged purities and yields were maintained around the maximum from 7.5 to 17.5 cm. Therefore, the optimal length of the upper-layer column was set to 15 cm, where the system pressure drop is minimized.

In the hybrid and serial double-layer SMBs, the system pressure drop is minimized where the upper- and lower-layer column diameters are the same, cf. eq 27. The minimum lengths of the upper-layer columns are 0.87 cm for separation cases 1 and 2 and 2.9 cm for separation cases 3 and 4. As the length of the upper-layer column increases, the diameter of the lower-layer column increases to maintain the same volume ratio. This means that the length of the upper-layer column that has a smaller diameter dominates the zone pressure drop and the system pressure drop increases as the length of the upper-layer column increases. As shown in Figure 6b−d, the averaged purities and yields are maintained around a maximum from 7.5 to 15 cm. With the same manner considered in the parallel double-layer SMB, the optimal length of the upper-layer column was set to 7.5 cm for separation cases 1 and 2 and 10 cm for separation cases 3 and 4.

4.2. Screening of Serial Column Connection in Paired Double-Layer Zones. In the hybrid and serial double-layer SMBs, the column pairs in the paired double-layer zones are connected in series so that there are two connection orders, the UL and LU connections, and four combinations, UL−UL, UL−LU, LU−UL, and LU−LU. The column pair in zone 5 moves to zone 4 and the connection is parallelized at the end of the port switching interval. The columns in zone 3U and 3L also move to zone 2 and form a serialized column pair. Therefore, the

https://doi.org/10.1021/acs.iecr.1c01268
Ind. Eng. Chem. Res. 2021, 60, 8911−8926

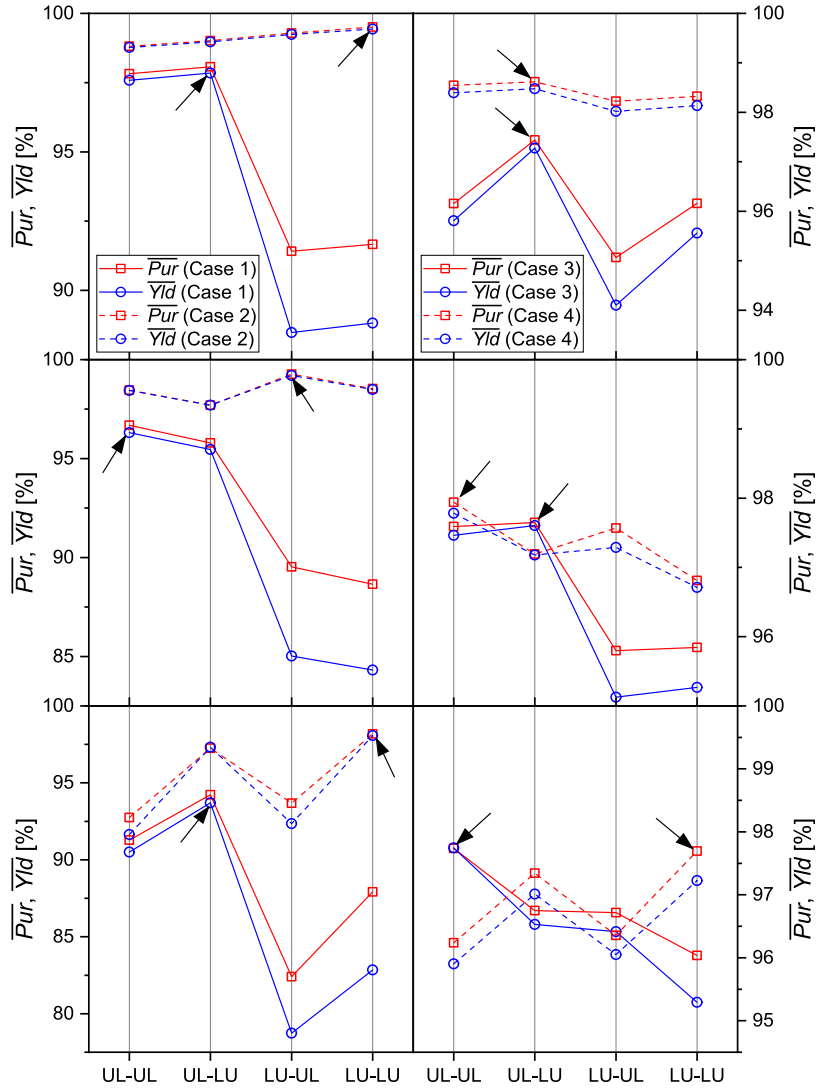

Figure 8. Screening of the serial connection of paired double-layer zones in terms of the average purity and yield. Upper, hybrid layer configuration; middle, serial-1 layer configuration; lower, serial-2 layer configuration; left sides, separation cases 1 and 2; right sides, separation cases 3 and 4; black arrows, chosen optimal serial column connections. Other design parameters were fixed to the standard values in Table 2.

connection order affects the performances of the hybrid and serial double-layer SMBs.

Figure 7 compares the internal concentration profiles of the hybrid double-layer SMBs with four different serial column connections in the paired double-layer zones at the end of the port switching interval of cyclic steady state. The outlet flows of zones 4U and 4L merge and enter the first column in zone 5. Where the UL connection is applied in zones 5 and 6 (Figure 7a,c), the first and last columns in zone 5 move to the upper layer and the lower layer of zone 4 at the end of the port switching interval, respectively. Therefore, the more-retained component that enters the first column in zone 5 cannot contaminate the intermediate stream if it does not penetrate the first column. This means that the first column in zone 5 inherits the role of zone 4U, and the intermediate-retained component should penetrate the last column in zone 5 to concentrate it in the intermediate port. Therefore, the effective volume of zone 5, which holds the intermediate-retained component to avoid raffinate port contamination, decreases, and the raffinate product can be easily contaminated compared to the parallel configuration.

On the contrary, the first column should not contain the more-retained component where the LU connection is applied in zone 5 (Figure 7b,d). The intermediate-retained component profile is not much spread on zone 5 because it is efficiently refluxed to zone 4L by switching the first column in zone 5 to zone 4L, and the entire volume of zone 5 is used to hold the intermediate-retained component. Therefore, it is easy to isolate the less-retained component in the raffinate port. However, the more-retained component that enters the first column in zone 5 contaminates the intermediate port immediately.

For the same reasons, the UL connection in zone 2 (Figure 7a,b) efficiently prevents the more-retained component from penetrating zone 3L, but the LU connection in zone 2 (Figure 7c,d) efficiently prevents the intermediate-retained component from contaminating the extract stream. Therefore, the UL connections in zones 2 and 5 provide good separation of the intermediate-retained component, but the intermediate-retained component may contaminate the extract and raffinate streams. On the contrary, the LU connections in zones 2 and 5 respectively provide good separations of the more- and less-retained components, but the more- and less-retained

https://doi.org/10.1021/acs.iecr.1c01268
Ind. Eng. Chem. Res. 2021, 60, 8911−8926

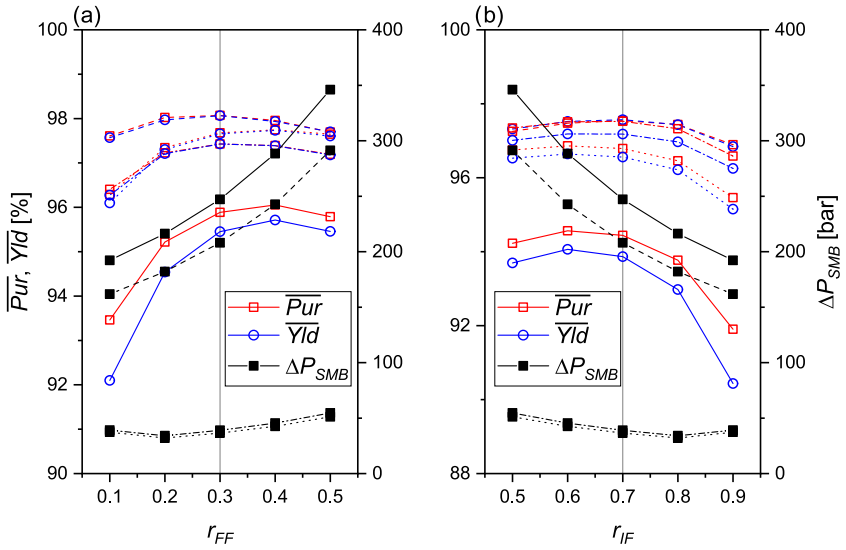

Figure 9. Screening of the flow-focusing ratio in terms of the average purity and yield and the pressure of the SMB system. (a) r_{FF} of serial-1 layer configuration and (b) r_{IF} of serial-2 layer configuration. Solid line, separation case 1; dashed line, separation case 2; dotted line, separation case 3; dash-dot line, separation case 4; and vertical gray lines, chosen optimal flow-focusing ratios. Other design parameters were fixed to the standard values in Table 2.

components may contaminate the intermediate stream. As opposed to the parallel column operation, the serial column connections in the paired double-layer zone can provide lopsided performance so that it may be a good alternative to the parallel column operation in specific cases, e.g., the UL connection in both zones 2 and 5 for a ternary separation with excessively high mass-transfer resistance of the most-retained component.

The serial column connections should be determined in consideration of separation difficulty, the ratio of the lower- to upper-layer volumes, and the efficiency of the columns. Therefore, the preferred serial column connections may be different in all separation cases. Figure 8 shows the averaged purity and yield changed by the serial column connections of the paired double-layer zones.

In separation case 1, large m-values were chosen for zones 2 and 3L (cf. Figure 2a). This means that the internal profile of the more-retained component can easily reach the intermediate port compared to separation case 2 so that the UL connection in zones 1 and 2 provides better averaged purity and yield (solid lines in the upper left plane of Figure 8). On the contrary, small m-values were chosen for zones 2 and 3L in separation case 2 (cf. Figure 2a). In this condition, the extract stream can be easily contaminated by the intermediate-retained component so that the LU connection in zones 1 and 2 provides slightly better performances. Since the less- and intermediate-retained component separation is more difficult than the more- and intermediate-retained component separation, it is difficult to avoid the contaminations of the intermediate and raffinate streams by changing the serial column connections in zones 5 and 6, and no significant differences are shown. In separation cases 3 and 4 (cf. Figure 2b), the more- and intermediate-retained component separation is more difficult than the less- and intermediate-retained component separation, but the difficulties are not significantly different. Therefore, the changes of the averaged purities and yields are in 4% ranges (the upper right plane of Figure 8).

In the serial double-layer SMBs (middle and lower planes of Figure 8), the feed or intermediate stream flows are focused in the middle of the port switching interval and the flow rates in the paired double-layer zones are correspondingly changed. This means that the internal concentration profiles are developed in intermittent feeding and withdrawal strategies with higher flow rates than those in the hybrid double-layer SMB. Therefore, the optimal serial column connections for the serial double-layer SMBs were different from the hybrid double-layer SMB. For each separation case, the optimal serial column connections of the hybrid and two serial double-layer SMBs were chosen (black arrows in Figure 8).

In the dA/dT/dG separation problem, the mass-transfer rate of the most-retained component dA is much smaller than others (cf. $k_{eff,i}$ in Table 1) and the flow rates of zones 2 and 3L were fast in separation case 1, i.e., the most-retained component can easily penetrate the intermediate port by band spreading. Therefore, the UL connections in zones 1 and 2 provided better performances in separation case 1, as discussed in Figure 7. In separation case 2, the spread band of the most-retained component was efficiently isolated by slow flow rates of zones 2 and 3L so that both UL and LU connections provided relatively similar product qualities. On the contrary, all components have similar mass-transfer resistance in the dT/dG/dC separation problem (separation cases 3 and 4) and the separation difficulties between the most- and intermediate-retained components and the intermediate- and least-retained components are similar to the dA/dT/dG separation problem. Narrow range changes of the product qualities were observed in separation cases 3 and 4.

4.3. Screening of Serialized Operation for Divided Double-Layer Zones. Two more design parameters—the ratio and position of the flow-focusing steps—should be determined in the serial double-layer SMBs. Since higher-zone flow rates are imposed where the intermediate stream flow is focused and the sum of the ratios of feed and intermediate flow-focusing steps ($r_{FF} + r_{IF}$) is 1, the ratio of feed flow-focusing step r_{FF} and the ratio of intermediate flow focusing r_{IF} were screened from 0.5 to 0.1 and from 0.5 to 0.9, respectively. As the ratio of feed flow focusing decreases, i.e., the ratio of intermediate flow focusing increases, the system pressure drop decreases (Figure

https://doi.org/10.1021/acs.iecr.1c01268
Ind. Eng. Chem. Res. 2021, 60, 8911−8926

Table 4. Comparisons of Various Layer Configurations of Double-Layer SMB in Terms of Average Process Performances and the System Pressure Drop with the Optimized Design Parameters and Port Switching Interval

sep. case	$L_{C,U}$ (cm)	layer conf.[a]	$r_{FF}(r_{IF})/s_{FF}(s_{IF})$	t_S (min)	$\overline{Pur}$ (%)	$\overline{Yld}$ (%)	$\overline{Pr} \times 10^3$ (g/(L h))	$\overline{DC}$ (L/g)	ΔP_{SMB} (bar)	$F_{Obj} \times 10^3$
1	15	P-P-P	N/A	18.7	97.4	97.0	50.3	59.0	3.87	0.159
	7.5	UL-P-LU	N/A	10.3	98.0	97.7	92.1	58.6	57.6	0.505
	7.5	UL-S1-UL	0.3/0.75	19.9	97.9	97.6	47.6	58.7	41.5	0.244
	7.5	UL-S2-LU	0.7/0.25	21.3	96.9	96.5	44.0	59.3	38.7	0.086
2	15	parallel	N/A	3.8	98.6	98.6	251	58.2	17.0	2.23
	7.5	LU-P-LU	N/A	3.7	98.6	98.5	258	58.2	133	2.27
	7.5	LU-S1-UL	0.3/0.75	4.8	98.8	98.7	199	58.1	142	1.91
	7.5	LU-S2-LU	0.7/0.25	6.6	98.7	98.6	145	58.2	103	1.33
3	15	parallel	N/A	5.2	97.8	97.6	234	19.5	6.71	3.41
	10	UL-P-LU	N/A	6.4	97.3	97.1	189	19.6	27.4	1.83
	10	UL-S1-LU	0.3/1.0	10.1	97.9	97.7	121	19.4	22.7	1.99
	10	UL-S2-UL	0.7/0.0	7.0	98.4	98.3	175	19.3	32.7	4.04
4	15	parallel	N/A	3.4	98.6	98.5	362	19.3	11.2	9.42
	10	UL-P-LU	N/A	5.8	98.0	97.8	211	19.4	32.4	3.69
	10	UL-S1-UL	0.3/1.0	5.7	98.6	98.5	216	19.3	43.1	5.74
	10	LU-S2-LU	0.7/0.0	12.8	97.7	97.3	94.9	19.5	19.2	1.23

[a]{Zones 1 and 2}-{zones 3 and 4}-{zones 5 and 6}; P, parallel; S1, serial-1; S2, serial-2; UL, upper-to-lower; LU, lower-to-upper.

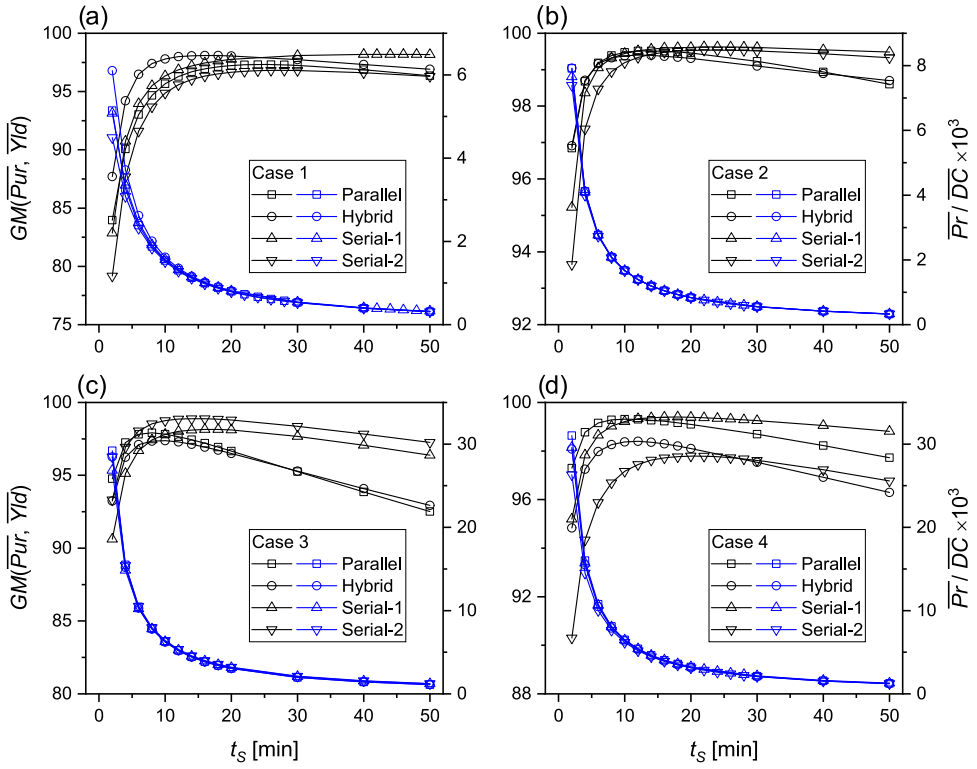

Figure 10. Changes in the product quality and process economy in terms of the port switching interval. (a) Separation case 1, (b) separation case 2, (c) separation case 3, and (d) separation case 4. Black lines and symbols, product quality, GM($\overline{Pur}$, $\overline{Yld}$); blue lines and symbols, process economy, $\overline{Pr}/\overline{DC}$.

9) because low-zone flow rates are imposed in the intermediate flow-focusing step. However, the upper and lower layers are individually operated in the corresponding steps so that narrow focusing of the feed flow (wide focusing of the intermediate flow) causes loss of efficiency in zones 3U and 4U due to fast zone flow rates. Eventually, the averaged purity and yield were maximized in $0.3 \le r_{FF} \le 0.4$ ($0.6 \le r_{IF} \le 0.7$) for all separation cases so that the ratio of feed flow focusing r_{FF} was set to 0.3 (r_{IF} = 0.7) for low system pressure drop.

The other design parameter, the position of the flow-focusing step, does not affect the system pressure drop, but it just specifies the pattern of the operation steps. The pattern of the operation steps was split into two distinct step operations, where the feed flow-focusing step is located in the middle of the port switching interval (serial-1) and the intermediate flow-focusing step is located in the middle of the port switching interval (serial-2). Since identical ratios of the flow-focusing steps were chosen for all separation cases, serial-1 step operations with s_{FF} = 0 and 1 are identical to serial-2 step operations with s_{IF} = 1 and 0. The

https://doi.org/10.1021/acs.iecr.1c01268
Ind. Eng. Chem. Res. 2021, 60, 8911−8926

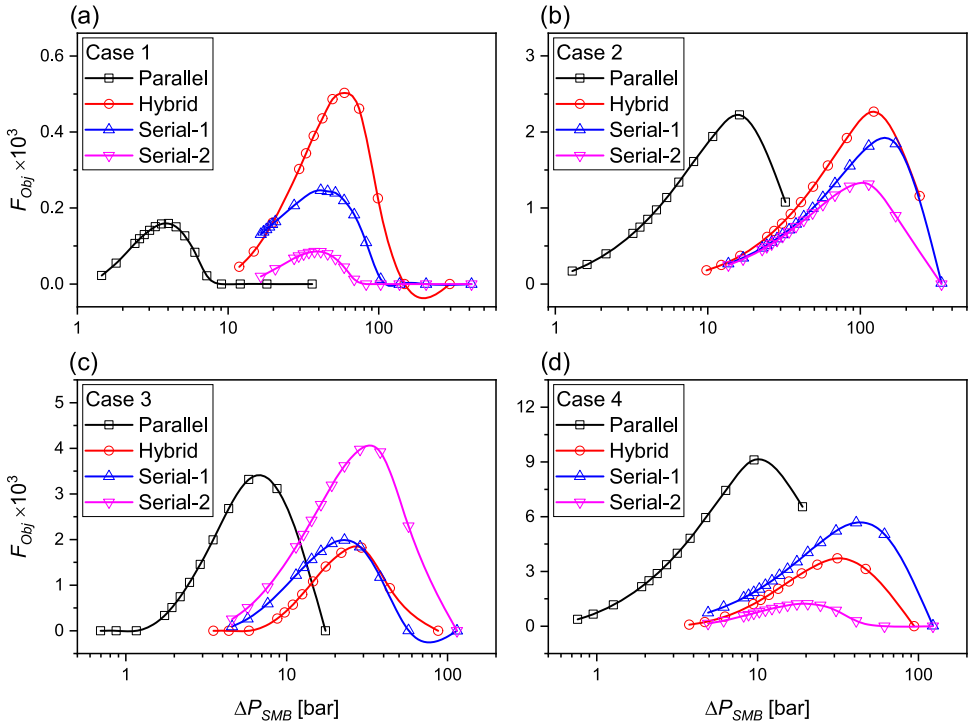

Figure 11. Changes of the objective function F_{Obj} in terms of the system pressure drop. (a) Separation case 1, (b) separation case 2, (c) separation case 3, and (d) separation case 4. Symbols, results from simulations; lines, natural cubic spline interpolation.

positions of the flow-focusing step were chosen where the averaged purity and yield were maximized. For separation cases 1 and 2, $s_{FF} = 0.75$ and $s_{IF} = 0.25$. For separation cases 3 and 4, $s_{FF} = 1.0$ and $s_{IF} = 0.0$.

4.4. Comparisons of Various Layer Configurations of Double-Layer SMB. In general, the column efficiency increases as the linear velocity of the mobile phase decreases due to the limited mass-transfer rate, but the column efficiency decreases as the linear velocity of the mobile phase increases due to increased residence time for axial dispersion. This means that the product quality, purity and yield, and the desorbent consumption have the maximum and the minimum at certain flow rates, respectively. The productivity increases as the feed throughput increases if the product quality is not significantly changed. Consequently, the process performances are radically changed by the zone flow rates, which are increased as the port switching interval is shortened at fixed operating points, *m*-values. Therefore, the port switching intervals of the double-layer SMBs should be optimized in the aspect of product quality and process economy. The optimized design parameters were used to screen the port switching interval, cf. Table 4.

Figure 10 shows the changes in the product quality, GM($\overline{\text{Pur}}$, $\overline{\text{Yld}}$), and the process economy, $\overline{\text{Pr}}/\overline{\text{DC}}$, in terms of the port switching interval. Since the desorbent consumptions were not radically changed in the range of investigated port switching intervals, 2−50 min, the process economies were exponentially increased as the port switching interval decreased. However, the product qualities were maximized at certain port switching intervals and radically decreased as the port switching interval decreased. Since the hybrid and serial double-layer SMBs have additional degrees of freedom compared to the parallel double-layer SMB, the product qualities of the hybrid and serial double-layer SMBs were better than those of the parallel double-layer SMB in certain separation cases. However, the product qualities of the hybrid and serial double-layer SMBs deviated from the product quality of the parallel double-layer SMB within ±5% point range. This means that the productivity dominantly increased by the feed throughput increment so that the process economies were almost the same in all separation cases.

To compare four different layer configurations of the double-layer SMBs in terms of process performances and the system pressure drops, the port switching intervals were optimized. Figure 11 shows the changes of the objective functions in terms of the system pressure drop. The system pressure drop is inversely proportional to the port switching interval, $\log(t_S) \propto -\log(\Delta P_{SMB})$. For separation cases 1 and 2, the system pressure drops of the hybrid and serial double-layer SMBs were approx. 10 times higher than those of the parallel double-layer SMB. However, the hybrid and serial double-layer SMBs could be operated in reduced system pressure drops, approx. 5 times higher than the hybrid double-layer SMB, because of the smaller volume ratio, r_V. To determine the optimum port switching interval, the trajectories of the objective functions were interpolated by the natural cubic spline interpolation and then the system pressure drops were converted to the port switching interval at maximum.

Table 4 compares the product qualities, process performances, and system pressure drops of four different layer configurations of the double-layer SMBs. Since the port switching interval was optimized corresponding to the objective function that was weighted by the averaged purity and yield, all layer configurations provide similar product qualities. However, the double-layer SMBs with serialized layer configurations, hybrid, serial-1, and serial-2, provide better performances than the parallel double-layer SMB in separation cases 1−3 and relatively similar performances compared to the parallel double-layer SMB in separation case 4. Even though the column dimensions and other design parameters were determined to reduce the system pressure drop, the serialized double-layer

https://doi.org/10.1021/acs.iecr.1c01268
Ind. Eng. Chem. Res. 2021, 60, 8911−8926

Table 5. Comparisons of the Structural and Operational Complexities of Eight-Zone SMB, SMB Cascade, and Various Layer Configurations of Double-Layer SMB with a Minimum Number of Columns

	structural						operational			
process	N_C	N_V	N_P	N_T	I_{SC}[a]	I_{SC}[b]	N_O	N_R	I_{OC}[a]	I_{OC}b[b]
eight-zone SMB	8	8 × 8	7	0	79	21.4	8	1	9	5
SMB cascade	8	8 × 4	8	1	49	20.2	8	2	10	6
parallel double-layer SMB	12	6 × 11	10	0	88	28.6	12	1	13	7
hybrid double-layer SMB	12	6 × 13	6	0	96	25.8	8	1	9	5
serial double-layer SMB	12	6 × 13	5	0	95	24.8	16	1	17	9

[a]Complexity indexes with the weighting factors equal to 1.0. [b]Complexity indexes with the adjusted weighting factors for an on−off valve and an operation, w_V = 0.1 and w_O = 0.5.

SMBs still generate higher system pressure drops than the parallel double-layer SMB. However, the differences are reduced to approx. 10-fold for separation cases 1 and 2 and 4-fold for separation cases 3 and 4 compared to the standard design parameter conditions described in Table 3. In separation cases 3 and 4, the step operations for the divided double-layer zones of serial-1 and serial-2 configurations are identical (s_{FF} = 1, s_{IF} = 0, and $r_{FF} = 1 - r_{IF}$), but different serial connections (e.g., UL-S1-UL and LU-S2-LU for separation case 4 in Table 4) were found as an optimum by the orthogonal parameter screening method. Since the design parameters, the serial column connections and the flow-focusing operations are mutually related and it is difficult to maintain the orthogonality (at least near-orthogonality), a detailed investigation for the optimal design of the serial double-layer SMBs is required.

Note that this optimization was carried out at fixed operating conditions with the simple parameter screening method. Therefore, it does not mean that those process performances were not fully optimized. However, it shows that the double-layer SMB with serialized layer configurations, which have simple internal flow patterns and are easy to be implemented, have the potential to substitute the parallel double-layer SMB if the system can be operated at high pressures. In previous work, the process performances were compared with the parallel double-layer SMB at the same operating conditions used in this work.[8] Therefore, the eight-zone SMB and the SMB cascade were included in the comparisons of the system complexities, the structural and operational complexities. As described in Table 5, the hybrid double-layer SMB needed the most complex process structure and the serial double-layer needed the most complex operation. Note that all weighting factors were presumed to be 1.0. In aspects of costs and operational difficulty, a pump should have a heavier weighting factor than an on−off valve. If a chromatographic process includes a recycle stream, the design and operating conditions should be carefully determined due to additional pressure increase and remixing of separated components. Therefore, the weighting factors for an on−off valve and an operation, w_V and w_O, were adjusted to 0.1 and 0.5, respectively. In these conditions, the structural and operational complexities of the double-layer SMBs were comparable to the early-established ternary SMBs and the hybrid and serial double-layer SMBs needed less complex process structures than the parallel double-layer SMB.

5. CONCLUSIONS

The parallel double-layer SMB that mimics the countercurrent flows of the dividing wall column in fractional distillation requires complex internal flow patterns to separate ternary mixtures. However, it is difficult to be realized in a real chromatographic process. Two alternative double-layer SMB concepts were introduced by applying serial connection of columns and serialized step operation. The alternative layer configurations provided comparable process performances at the chosen ternary separation problems, but relatively high system pressure drops were generated compared to the parallel double-layer SMB. In the aspect of process structure, the serialized layer configurations could provide advantages without significant loss of process performances but bearing high system pressure drop.

AUTHOR INFORMATION

Corresponding Author

Ju Weon Lee − *Institute for Automation Engineering, Otto-von-Guericke University, 39106 Magdeburg, Germany; Max-Planck-Institute for Dynamics of Complex Technical Systems, 39106 Magdeburg, Germany;* orcid.org/0000-0002-1459-1038; Phone: +49 391 6110392; Email: ju.lee@ovgu.de, lee@mpi-magdeburg.mpg.de; Fax: +49 391 6110521

Complete contact information is available at: https://pubs.acs.org/10.1021/acs.iecr.1c01268

Notes

The author declares no competing financial interest.

ACKNOWLEDGMENTS

This research was funded by the Deutsche Forschungsgemeinschaft (DFG, German Research Foundation)—grant LE 4481/2-1, project number 441831362.

REFERENCES

(1) Broughton, D. B.; Neuzil, R. W.; Pharis, J. M.; Brearley, C. S. The parex process for recovering paraxylene. *Chem. Eng. Prog.* **1970**, *66*, 70.

(2) Kim, K.-M.; Lee, J. W.; Kim, S.; Santos da Silva, F. V.; Seidel-Morgenstern, A.; Lee, C.-H. Advanced Operating Strategies to Extend the Applications of Simulated Moving Bed Chromatography. *Chem. Eng. Technol.* **2017**, *40*, 2163.

(3) Sá Gomes, P.; Rodrigues, A. E. Outlet streams swing (OSS) and multifeed operation of simulated moving beds. *Sep. Sci. Technol.* **2007**, *42*, 223.

(4) Katsuo, S.; Mazzotti, M. Intermittent simulated moving bed chromatography: 1. Design criteria and cyclic steady-state. *J. Chromatogr. A* **2010**, *1217*, 1354.

(5) Lee, J. W.; Kienle, A.; Seidel-Morgenstern, A. On-line optimization of four-zone simulated moving bed chromatography using an equilibrium-dispersion model: I. Simulation study. *Chem. Eng. Sci.* **2020**, *225*, No. 115810.

(6) Nowak, J.; Antos, D.; Seidel-Morgenstern, A. Theoretical study of using simulated moving bed chromatography to separate intermediately eluting target compounds. *J. Chromatogr. A* **2012**, *1253*, 58.

(7) Wankat, P. C. Simulated moving bed cascades for ternary separations. *Ind. Eng. Chem. Res.* **2001**, *40*, 6185.
(8) Lee, J. W. Expanding simulated moving bed chromatography into ternary separations in analogy to dividing wall column distillation. *Ind. Eng. Chem. Res.* **2020**, *59*, 9619.
(9) Storti, G.; Mazzotti, M.; Morbidelli, M.; Carrà, S. Robust design of binary countercurrent adsorption separation processes. *AIChE J.* **1993**, *39*, 471.
(10) Bird, R. B.; Stewart, W. E.; Lightfoot, E. N. *Transport Phenomena*; John Wiles & Sons: New York, 1960.
(11) Abel, S.; Bäbler, M. U.; Arpagaus, C.; Mazzotti, M.; Stadler, J. Two-fraction and three-fraction continuous simulated moving bed separation of nucleosides. *J. Chromatogr. A* **2004**, *1043*, 201.
(12) Paredes, G.; Abel, S.; Mazzotti, M.; Morbidelli, M.; Stadler, J. Analysis of a simulated moving bed operation for three-fraction separations (3F-SMB). *Ind. Eng. Chem. Res.* **2004**, *43*, 6157.
(13) Rumble, J. R. *CRC Handbook of Chemistry and Physics*, 99th ed.; CRC Press: Boca Raton, 2018.
(14) Burden, R. L.; Faires, J. D. *Numerical Analysis*, 5th ed.; PWS Publishing: Boston, 1993.
(15) Lee, J. W.; Wankat, P. C. Optimized design of recycle chromatography to isolate intermediate retained solutes in ternary mixtures: Langmuir isotherm systems. *J. Chromatogr. A* **2009**, *1216*, 6946.

https://doi.org/10.1021/acs.iecr.1c01268
Ind. Eng. Chem. Res. 2021, 60, 8911−8926